

# Integral-Type Event-Triggered Receding Horizon Control of Nonlinear Systems with Additive Disturbance

Qi Sun, *Student Member, IEEE*, Jicheng Chen, *Student Member, IEEE*,  
Yang Shi, *Fellow, IEEE*

## Abstract

This paper studies the event-triggered receding horizon control (RHC) of continuous-time nonlinear systems. An integral-type event-triggered mechanism is proposed to save the communicational resource, and a less conservative robustness constraint is introduced to the RHC scheme for compensating the additive disturbance. Based on these formulations, the designed event-triggered algorithm is shown to have better performance on avoiding unnecessary communication. Furthermore, the feasibility of the integral-type event-triggered RHC scheme and the stability of the closed-loop system are rigorously investigated. Several sufficient conditions to guarantee these properties are established, which indicate that a trade-off exists for designing parameters such as the prediction horizon, the disturbance bound, the triggering level, and the contraction rate for the robustness constraint. The effectiveness of the proposed algorithm is illustrated by a numerical example.

## Index Terms

Nonlinear receding horizon control, integral-type event-triggered mechanism, continuous-time nonlinear system, robust control.

## I. INTRODUCTION

Recent research interests and efforts have been directed towards reducing the computation or/and communication load in control systems by using the event-triggered scheme. This control paradigm employs the so-called event-triggered mechanism (ETM) to avoid unnecessary

The authors are with the Department of Mechanical Engineering, University of Victoria, Victoria, BC V8W 2Y2, Canada (e-mail: sunqi@uvic.ca; jichengc@uvic.ca; yshi@uvic.ca).

communication. Compared with the conventional periodic control, event-triggered control treats sampling instants as a design parameter while the periodic scheme samples the states at fixed time instants. The event-triggered paradigm is mainly to design a scheduling mechanism with the capability of determining when the states or sensor outputs should be sampled. The benefit of using this method is that it can provide a smaller communication rate and thus reduce the communication load, especially in cases where the computation and communication resources are scarce. Therefore the event-triggered control scheme has been widely studied under such resource-limited scenarios [1]–[7].

Several pioneering works have been devoted to build the fundamental blocks of the event-triggered control [1]–[4]. The works [1]–[3] used a constant threshold-based event-triggered scheme, which enable the next sampling when the norm of state or estimation error exceeds a certain constant bound. Compared with the conventional periodic control, this method is shown to have great advantages in terms of reducing communication rate [1]. In another early work [4], the proposed event-triggered scheme adopted a so-called relative threshold policy for a class of nonlinear systems, where it allows transmissions when the norm of measurement error exceeds a weighted norm of the state. In addition, a lower bound for inter-execution time is proved to exist for avoiding the Zeno behavior. The study of state-based event-triggered control can be found in [3], [5], [8], and output-based event-triggered control has been reported in [9]. In [7], the authors proposed a periodic event-triggered scheme for reducing the communication rate, where the event-triggering condition is checked periodically with a fixed time interval. To further reduce the communication rate, the authors in [10] proposed a novel integral-based event-triggered scheme by incorporating the integral of estimated errors to the event-triggering condition.

In control research area, Receding Horizon Control (RHC) has been one of the most successful control methodologies. The basic idea of RHC framework is to solve optimization problems online at each sampling instant, and apply the corresponding control action to the plant. In particular, introducing event-triggered scheme to RHC is of great importance in term of alleviating communication load, thus receives many research studies [11]–[16]. By using the event-triggered scheme, the event-triggered RHC can avoid unnecessary communication, and thus reduce the frequency of solving heavy computational optimization problems. Therefore, employing event-triggered scheme on RHC is preferable in term of saving computational cost. Some research has been concentrated on event-triggered RHC of linear systems [11], [12]. The

authors in [12] studied the event-triggered RHC of linear systems with additive disturbance by using a tube-based approach. There have been also research interests focused on nonlinear systems [13]–[15]. In [13], an event-triggered scheme was proposed for nonlinear systems with additive disturbance by continuously measuring the error between the actual and the predicted trajectories. In order to acquire the benefit of avoiding Zeno behavior, the authors in [14] proposed an event-triggered mechanism design which can guarantee that the inter-execution time is lower bounded. Event-triggered RHC can also be found in decentralized and networked control systems [15], [17]. In [15], an event-triggered RHC framework was proposed for stabilizing the distributed nonholonomic systems. However, such RHC-based event-triggered schemes only use the instantaneous information of the actual and predicted state. The integral of the error between actual and predicted trajectories can be used in the event-triggered RHC framework for further reducing the communication rate compared with the existing results.

In this paper, we investigate the robust integral-type event-triggered RHC problem for the continuous-time nonlinear systems with additive disturbance, aiming at alleviating the computational load while ensuring the feasibility of proposed RHC problem and the stability of the closed-loop system. The main contributions of this work are three-fold:

- An integral-type event-triggered RHC algorithm has been designed for the continuous-time nonlinear system in the presence of additive disturbance. This ETM is proposed by using the integral of the error between the actual and predicted states. By using the ETM, the optimization problem will be only solved when the accumulated error reaches the designed triggering level. The triggering level is also designed to avoid the Zeno behavior;
- A novel robustness constraint is proposed to compensate the additive disturbance for the closed-loop system. The nominal state in the optimization problem is required to satisfy a time-varying constraint, which is decreasing proportionally to time. Moreover, this constraint will shrink into an ellipsoidal terminal region after a prediction horizon. By using this unique configuration, the optimization problem admits a less conservative initial feasible region.
- The feasibility of the integral event-triggered RHC and the stability of the closed-loop systems are thoroughly studied. Sufficient conditions for ensuring the feasibility and stability are provided, respectively. It is also shown that the feasibility and stability conditions are subject to the prediction horizon, the bound of disturbance, the triggering level, and the contraction rate for the robustness constraint. Moreover, there exists a design trade-off for the parameters when the control performance and the computational load are considered.

The paper is organized as follows: Section II describes the problem formulation of the proposed event-triggered RHC algorithm. Section III states the feasibility and stability results of the proposed algorithm. Section IV gives a simulation example to verify the effectiveness and computational efficiency of the proposed algorithm.

**Notations:** The real space is denoted by  $\mathbb{R}$  and the symbol  $\mathbb{N}$  represents the set of all positive integers. For a given matrix  $X$ , we use  $X^\top$  and  $X^{-1}$  to denote its transpose and inverse. For a symmetric matrix  $S \in \mathbb{R}^{n \times n}$ , we write  $S \succ 0$  or  $S \succeq 0$  if  $S$  is positive definite (PD) or positive semidefinite (PSD). The largest and smallest eigenvalues of  $S$  are denoted by  $\bar{\lambda}(S)$  and  $\underline{\lambda}(S)$ , respectively. Given a column vector  $x \in \mathbb{R}^n$ ,  $\|x\|$  represents its Euclidean norm, and  $\|x\|_P := \sqrt{x^\top P x}$  is the  $P$ -weighted norm. We also use the notation  $\|x\|_P^2 := x^\top P x$ . Given a continuously differentiable vector-valued function  $g(t)$  on  $[a, b]$ , we use  $g'(t)$  to represent its Jacobian matrix.

## II. PROBLEM FORMULATION

### A. System Dynamics and Optimization Problem

We consider a continuous-time nonlinear system with additive disturbance as follows

$$\dot{x}(t) = f(x(t), u(t)) + \omega(t), \quad (1)$$

where  $x(t) \in \mathbb{R}^n$  is the state variable,  $u(t) \in \mathbb{R}^m$  is the control input, and  $\omega(t) \in \mathbb{R}^n$  is the additive disturbance. The system satisfies  $f(0, 0) = 0$  and has a Lipschitz constant  $L$ . The control input  $u(t) \in \mathcal{U}$ , where  $\mathcal{U} \in \mathbb{R}^m$  is a compact set containing the origin. Moreover, the disturbance  $\omega(t)$  is also in a compact set  $\mathcal{W}$  containing the origin, which is bounded by  $\rho \triangleq \sup_{\omega(t) \in \mathcal{W}} \|\omega(t)\|$ . By linearizing the nonlinear system (1) at the equilibrium  $(0, 0)$ , we can obtain the linearized state-space model:

$$\dot{x}(t) = Ax(t) + Bu(t) + \omega(t), \quad (2)$$

where  $A = \frac{\partial f}{\partial x}|_{(0,0)}$  and  $B = \frac{\partial f}{\partial u}|_{(0,0)}$ .

In the following, we introduce a conventional assumption for the linearized model (2), which is necessary for analyzing the closed-loop performance of the nonlinear system (1).

**Assumption 1.** *There exists a feedback control law  $u(t) = Kx(t)$  such that the closed-loop system matrix  $A + BK$  is Hurwitz.*

In addition, we also make use of a conventional result of the control invariant property of the nonlinear system (1).

**Lemma 1.** [18] *If  $f : \mathbb{R}^n \times \mathbb{R}^n \rightarrow \mathbb{R}^n$  is twice continuously differentiable,  $f(0, 0) = 0$ ,  $u(t)$  is piece-wise right-continuous and suppose that Assumption 1 holds, then given a stabilizable  $K$ , and two symmetric positive-definite matrices  $Q$  and  $R$ , there exists a constant  $\kappa > 0$  such that: (1) The Lyapunov equation  $(A + BK + \kappa I)^\top P + P(A + BK + \kappa I) = -Q^*$  admits a unique solution  $P \succ 0$ , where  $Q^* = Q + K^\top RK \in \mathbb{R}^{n \times n}$  and  $\kappa$  satisfies  $\kappa < -\bar{\lambda}(A + BK)$ ; (2)  $u(t) = Kx(t) \in \mathcal{U}$  and  $\Omega(\epsilon) := \{x \in \mathbb{R}^n \mid \|x\|_P^2 \leq \epsilon\}$  is control invariant by the feedback control law  $u(t) = Kx(t)$  for the nonlinear system (1).*

The nominal system of (1) can be defined as

$$\dot{\hat{x}}(s) = f(\hat{x}(s), \hat{u}(s)), \quad (3)$$

where  $\hat{x}(s)$  and  $\hat{u}(s)$  are the predicted states and control sequence, respectively. Note that the nominal system dynamics (3) will be used for constructing the equality constraint of the following optimization problem. In order to avoid ambiguity, we take explicit notations  $\hat{x}(s; t_k)$  and  $\hat{u}(s; t_k)$  for the predicted state and control trajectory at the  $k$ th event-triggered instant  $t_k$ . It should be noticed that the event-triggered instants are generated by using the integral-type ETM, which will be elaborated after introducing the optimization control problem.

Then the nonlinear optimization problem  $\mathcal{P}$  can be formulated as

$$\hat{u}^*(s; t_k) = \arg \min_{\hat{u} \in \mathcal{U}} J(\hat{x}(s; t_k), \hat{u}(s; t_k)) \quad (4)$$

$$\text{s.t. } \dot{\hat{x}}(s; t_k) = f(\hat{x}(s; t_k), \hat{u}(s; t_k)), \quad (5)$$

$$\hat{u}(s; t_k) \in \mathcal{U}, \quad s \in [t_k, t_k + T], \quad (6)$$

$$\|\hat{x}(s; t_k)\|_P \leq \frac{(t_k + T - s)M + s - t_k}{T} \alpha \epsilon. \quad (7)$$

The cost function is defined as follows

$$\begin{aligned} J(\hat{x}(s; t_k), \hat{u}(s; t_k)) \triangleq & \int_{t_k}^{t_k+T} \|\hat{x}(s; t_k)\|_Q^2 + \|\hat{u}(s; t_k)\|_R^2 \mathbf{d}s \\ & + \|\hat{x}(t_k + T, t_k)\|_P^2, \end{aligned} \quad (8)$$

where  $Q \succeq 0$ ,  $R \succ 0$ ,  $\mathbf{I}_n$  is the  $n \times n$  identity matrix,  $P$  is defined by using the method from Lemma 1,  $T$  is the prediction horizon,  $\epsilon$  is the designed parameter for defining the terminal set,

$\alpha \in (0, 1)$  is the scaling ratio, and  $M$  is the contraction rate for the robustness constraint (7). It should be noted that the terminal constraint is  $\Omega(t_k + T) = \alpha\epsilon$ .

By using the aforementioned system dynamics and optimization problem, we construct the following closed-loop system as

$$\dot{x}(t) = f(x(t), \hat{u}^*(t - t_k; t_k)) + \omega(t), \quad k \in \{0, 1, 2, \dots\}, \quad (9)$$

where  $t_k$  is the  $k$ th event-triggered instant. In this control framework, we use the optimal control sequence as the control input generated by solving the nonlinear optimization problem (4). In order to reduce the communication between the controller and the actuator, we take an integral-type ETM for determining when the next optimization should be conducted, i.e. solving the optimization problem and transmitting the optimal control sequence to the actuator.

**Remark 1.** *In the optimization problem (4), the robustness constraint (7) is used for compensating the additive disturbance when applying the optimal control sequence to the closed-loop system (9). The shrinking constraint-based method for robust RHC has been firstly used in [19]. In their configuration, the robustness constraint shrinks very fast to the terminal constraint as time evolves. In our approach, a less conservative constraint is proposed, where the shrinking rate is a constant. Intuitively, our proposed robustness constraint will provide a larger feasible set for solving the optimization problem.*

### B. Integral-type Event-triggered Mechanism

For the nonlinear system (1), we assume that the event-triggered instants set is  $\{t_0, t_1, \dots, t_k, \dots\}$  with  $t_{k+1} = t_k + h$ , where  $h$  is determined by the proposed event-triggered scheme (10). We also make the assumption that there is no time delay and inaccuracy when transmitting the sensor measurements to the digital controller. By using this configuration, an integral-type ETM is introduced for scheduling and implementing the sampling tasks, i.e. determining the event-triggered instants  $t_k$ . As shown in Fig. 1, the ETM produces an ON/OFF signal to the sensor by measuring the error between the actual state and the predicted optimal state. Based on this configuration, we can acquire the benefit of reducing both the computational and communicational load. The integral-type event-triggering condition is designed as

$$\begin{aligned} \bar{t}_{k+1} &= \inf_{h > t_k} \left\{ h : \int_{t_k}^{t_k+h} \|x(s; t_k) - x^*(s; t_k)\|_P ds = \delta \right\}, \\ t_{k+1} &= \min\{\bar{t}_{k+1}, t_k + T\}, \end{aligned} \quad (10)$$

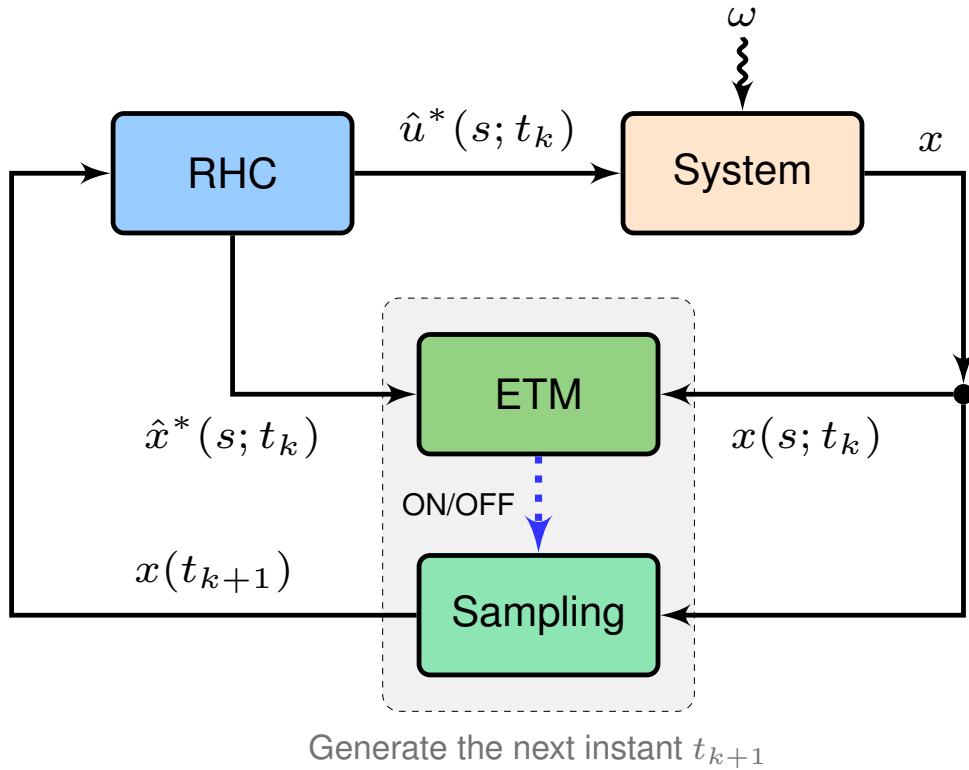


Fig. 1. The block diagram for event-triggered RHC.

where  $h$  is a minimum time instant satisfying the triggering condition (10). This ETM can take account of accumulated error between the measured state and optimal predicted state generated by the RHC algorithm (4) over the current period  $t_{k+1} - t_k$ , which is different from the event-triggered setting in [14]. The following theorem shows some important properties of the proposed integral-type ETM.

**Theorem 1.** *For the nonlinear system (1), if the event-triggered time instants  $t_k, k \in \mathbb{N}$  are implemented as (10), then the following result holds: The upper bound for inter-execution time is  $\sup_{k \in \mathbb{N}}(t_{k+1} - t_k) = T$ ; the lower bound  $\inf_{k \in \mathbb{N}}(t_{k+1} - t_k) = \beta T$  can be guaranteed by properly designing the triggering level  $\delta$  as*

$$\delta = \rho \bar{\lambda}(\sqrt{P}) \left[ e^{L\beta T} \left( \frac{\beta T}{L} - \frac{1}{L^2} \right) + \frac{1}{L^2} \right], \quad (11)$$

where  $\beta \in (0, 1)$  is a scaling parameter.

*Proof.* This proof can be done by two steps.

Step 1: The upper bound of inter-execution intervals is  $T$ . From the design of the integral-type ETM, it can be directly deduced that all the intervals  $t_{k+1} - t_k$  is less than or equal to the prediction horizon  $T$ .

Step 2: The lower bound for inter-execution intervals can be designed as  $\beta T$ . To prove this result, we firstly consider the upper bound for  $\|x(s; t_k) - x^*(s; t_k)\|_P$  at  $t_k$ . We assume here that the sensor measurements of the states are accurate, thus it follows that  $x(t_k; t_k) - x^*(t_k; t_k) = 0$ . By using the triangle inequality, we have  $\|x(s; t_k) - x^*(s; t_k)\|_P \leq \|x(t_k; t_k) - x^*(t_k; t_k) + \int_{t_k}^s \dot{x}(\tau; t_k) - \dot{x}^*(\tau; t_k) d\tau\|_P \leq \int_{t_k}^s L \|x(\tau; t_k) - x^*(\tau; t_k)\|_P + \|\omega(\tau)\|_P d\tau \leq \int_{t_k}^s L \|x(\tau; t_k) - x^*(\tau; t_k)\|_P d\tau + \rho \bar{\lambda}(\sqrt{P})(s - t_k)$ . Then by applying the integral form of Gronwall-Bellman inequality, it can be obtained that  $\|x(s; t_k) - x^*(s; t_k)\|_P \leq \rho \bar{\lambda}(\sqrt{P})(s - t_k) e^{L(s-t_k)}$ . Substituting the previous inequality to (10), we can deduce that  $\int_{t_k}^{t_{k+1}} \|x(s; t_k) - x^*(s; t_k)\|_P ds \leq \int_{t_k}^{t_{k+1}} \rho \bar{\lambda}(\sqrt{P})(s - t_k) e^{L(s-t_k)} ds = \rho \bar{\lambda}(\sqrt{P}) [e^{L(t_{k+1}-t_k)} (\frac{t_{k+1}-t_k}{L} - \frac{1}{L^2}) + \frac{1}{L^2}]$ . Since  $\bar{\lambda}(\sqrt{P})(s - t_k) e^{L(s-t_k)}$  is strictly larger than zero for  $s > t_k$ , we can choose  $\delta$  as (11) by setting  $t_{k+1} - t_k = \beta T$ . Therefore, it can be guaranteed that the lower bound of the triggered time interval is  $\inf_{k \in \mathbb{N}} (t_{k+1} - t_k) = \beta T$ . The proof is completed.  $\square$

**Remark 2.** Note that the designed ETM is based on the integral of the error between actual states and predicted states. The main difference of the integral-type ETM is that the accumulated error between two consecutive event-triggered instants is taken into account. It is worthwhile to point out that this event-triggered scheme is only valid for the system in the presence of disturbance.

### III. MAIN RESULTS

#### A. Feasibility Analysis

Following a conventional setup for RHC framework, we construct a classical feasible control sequence for the optimization problem (4). This same control policy has been widely exploited by [20], [21], and it can be given as

$$\tilde{u}(s; t_k) = \begin{cases} \hat{u}^*(s; t_{k-1}), & \text{if } s \in [t_k, t_{k-1} + T] \\ Kx(s; t_k), & \text{if } s \in [t_{k-1} + T, t_k + T] \end{cases} \quad (12)$$

Then the sub-optimal feasible control and state trajectory evolves as

$$\dot{\tilde{x}}(s; t_k) = f(\tilde{x}(s; t_k), \tilde{u}(s; t_k)). \quad (13)$$



Before presenting the result of this section, we would like to introduce a lemma which will be used in the following analysis.

**Lemma 2.** *Given a continuously differentiable vector-valued function  $g(t)$  on  $[a, b]$ , then the following inequality holds*

$$\sup_{t \in [a, b]} \|g(t)\| \leq \frac{1}{2} \int_a^b \|g'(t)\| dt + \frac{1}{2} \|g(a) + g(b)\|. \quad (14)$$

*Proof.* For every  $t \in [a, b]$ , we have two results:  $g(t) = g(a) + \int_a^t g'(\tau) d\tau$ ,  $g(b) = g(t) + \int_t^b g'(\tau) d\tau$ . Subtracting the aforementioned two equations, it yields  $2g(t) = g(a) + g(b) + \int_a^t g'(\tau) d\tau + \int_b^t g'(\tau) d\tau$ . By employing the triangle inequality, we can deduce from the above equality that  $\|g(t)\| \leq \frac{1}{2} \|g(a) + g(b)\| + \frac{1}{2} \int_a^t \|g'(\tau)\| d\tau + \frac{1}{2} \int_t^b \|g'(\tau)\| d\tau = \frac{1}{2} \int_a^b \|g'(t)\| dt + \frac{1}{2} \|g(a) + g(b)\|$ . Since every  $g(t)$  defined on the closed interval  $[a, b]$  is equal or less than the right side of the above inequality, thus the result (14) holds.  $\square$

To simplify the analysis of integral-type event-triggered configuration, we make use of a term  $e(s; t_k) = \tilde{x}(s; t_k) - \hat{x}^*(s; t_{k-1})$  for  $s \in [t_k, t_{k-1} + T]$ , which can be found continuously differentiable. Note that  $\tilde{x}(s; t_k)$  is defined as the candidate state trajectory generated by the nominal system (13), and  $\hat{x}^*(s; t_{k-1})$  is the solution of the optimization problem (4). In addition, we let the sub-optimal feasible state  $\tilde{x}(t_k; t_k) = x(t_k)$  by sampling the state at the  $k$ th triggered time instant  $t_k$ . For convenience, we denote  $g(s; t_k) = \sqrt{P}e(s; t_k)$ , where  $\sqrt{P}$  is the square root of the  $P$ . Then we can propose the following result.

**Corollary 1.** *Given  $e(s; t_k)$  and  $g(s; t_k)$  defined on  $s \in [t_k, t_{k-1} + T]$ , the following inequality holds*

$$\sup_{s \in [t_k, t_{k-1} + T]} \|e(s; t_k)\|_P \leq \frac{L^2 \beta T}{L \beta T - 1} e^{L(1-\beta)T} \delta. \quad (15)$$

*Proof.* By Lemma 2, we can obtain that

$$\begin{aligned} \sup_{s \in [t_k, t_{k-1} + T]} \|\sqrt{P}e(s; t_k)\| &\leq \frac{1}{2} L \int_{t_k}^{t_{k-1} + T} \|\sqrt{P}e(s; t_k)\| ds \\ &+ \frac{1}{2} \|\sqrt{P}e(t_k; t_k) + \sqrt{P}e(t_{k-1} + T; t_k)\|. \end{aligned} \quad (16)$$

Note that  $\|e(s; t_k)\|_P = \|\sqrt{P}e(s; t_k)\|$ , then it can be deduced from the above inequality that

$$\begin{aligned} \sup_{s \in [t_k, t_{k-1}+T]} \|e(s; t_k)\|_P &\leq \frac{1}{2}L \int_{t_k}^{t_{k-1}+T} \|e(s; t_k)\|_P \mathbf{d}s \\ &+ \frac{1}{2} \|2e(t_k; t_k) + \int_{t_k}^{t_{k-1}+T} \dot{e}(s; t_k) \mathbf{d}s\|_P \\ &\leq L \int_{t_k}^{t_{k-1}+T} \|e(s; t_k)\|_P \mathbf{d}s + \|e(t_k; t_k)\|_P. \end{aligned} \quad (17)$$

Next we show that the upper bound of  $\|e(t_k; t_k)\|_P$  is related to the triggering level  $\delta$ . By using the result from Theorem 1, the upper bound of  $\|e(s; t_k)\|_P$  is  $\rho\bar{\lambda}(\sqrt{P})(s - t_{k-1})e^{L(s-t_{k-1})}$  for  $s \in [t_{k-1}, t_k]$ . Thus, it can be obtained that  $\|e(h; t_k)\|_P \geq \|e(s; t_k)\|_P$  for  $s \in [t_{k-1}, t_k]$ . Note that we also have  $\delta = \rho\bar{\lambda}(\sqrt{P}) [e^{Lh} (\frac{h}{L} - \frac{1}{L^2}) + \frac{1}{L^2}]$  for  $h \in [\beta T, T]$ , where the triggering level  $\delta$  is designed as the integral of  $\|e(s; t_k)\|_P$  from  $t_{k-1}$  to  $t_{k-1} + h$ . By following simple calculation, we can obtain that

$$\rho\bar{\lambda}(\sqrt{P}) \left[ e^{Lh} \left( h - \frac{1}{L} \right) + \frac{1}{L} \right] = L\delta, \quad (18)$$

and consequently it follows that

$$\|e(h; t_k)\|_P \leq \rho\bar{\lambda}(\sqrt{P}) e^{Lh} h \leq L\delta \frac{h}{h - \frac{1}{L}}, \quad (19)$$

where  $L\beta T > 1$ . Since the function  $\frac{h}{h - \frac{1}{L}}$  gets its maximum at  $h = \beta T$ , the above inequality becomes

$$\|e(t_k; t_k)\|_P \leq \|e(h; t_k)\|_P \leq \frac{L^2\beta T}{L\beta T - 1} \delta. \quad (20)$$

According to Gronwall-Bellman inequality, one can obtain (15) by substituting (20) to (17). The proof is thus completed.  $\square$

Now we can analyze the iterative feasibility of the RHC problem (4), implying that if the RHC problem admits a solution at current time instant then a feasible solution exists for the next time instant. To prove this result, we use a conventional feasible control sequence candidate  $\tilde{u}(s; t_k)$  at time instant  $t_k$  defined in (12), where  $\tilde{u}(s; t_k) = \hat{u}^*(s; t_{k-1})$  for  $s \in [t_k, t_{k-1} + T]$  and  $\tilde{u}(s; t_k) = K\tilde{x}(s; t_k)$  for  $s \in [t_{k-1} + T, t_k + T]$ . In the following theorem, we will show that the designed control sequence candidate  $\tilde{u}(s; t_k)$  can steer the feasible state  $\tilde{x}(s; t_k)$  into  $\Omega(\alpha\epsilon)$  if some conditions can be satisfied. In addition, it is also necessary to show that the candidate state  $\tilde{x}(s; t_k)$  will remain in the designed state constraint (7).

**Assumption 2.** The optimization problem (4) admits a feasible solution  $\hat{u}^*(s; t_0)$  for the initial time  $t_0$ .

**Theorem 2.** Suppose that the Assumptions 1 and 2 hold. The RHC problem (4) is iteratively feasible under the following conditions:

$$\frac{L^2\beta T e^{L(1-\beta)T}}{L\beta T - 1} \rho \bar{\lambda}(\sqrt{P}) \left[ e^{L\beta T} \left( \frac{\beta T}{L} - \frac{1}{L^2} \right) + \frac{1}{L^2} \right] \leq (1 - \alpha)\epsilon, \quad (21)$$

$$T \geq -2 \frac{\bar{\lambda}(P)}{\underline{\lambda}(Q^*)\beta} \ln \alpha, \quad (22)$$

$$M \geq \max \left\{ \frac{L^2\beta T e^{L(1-\beta)T}}{L\beta T - 1} \frac{\delta}{\alpha\epsilon} + 1, 1 - \frac{1}{\beta} + \frac{1}{\alpha\beta} \right\}. \quad (23)$$

Moreover, the maximum allowable disturbance can be given as

$$\rho \leq \frac{(1 - \alpha)\epsilon}{\frac{L^2\beta T e^{L(1-\beta)T}}{L\beta T - 1} \bar{\lambda}(\sqrt{P}) \left[ e^{L\beta T} \left( \frac{\beta T}{L} - \frac{1}{L^2} \right) + \frac{1}{L^2} \right]}. \quad (24)$$

*Proof.* First, we show that the designed control sequence  $\tilde{u}(s; t_k)$  for  $s \in [t_k, t_{k-1} + T]$  drives  $\tilde{x}(s; t_k)$  into  $\Omega(\epsilon)$ , i.e.  $\|\tilde{x}(s; t_k)\|_P \leq \epsilon$ . Let us construct an error norm  $\|\tilde{x}(s; t_k) - \hat{x}^*(s; t_{k-1})\|_P$  for  $s \in [t_k, t_{k-1} + T]$ . By using Corollary 1, we can obtain that

$$\sup_{s \in [t_k, t_{k-1} + T]} \|\tilde{x}(s; t_k) - \hat{x}^*(s; t_{k-1})\|_P \leq \frac{L^2\beta T}{L\beta T - 1} e^{L(1-\beta)T} \delta. \quad (25)$$

Then it follows that  $\|\tilde{x}(t_{k-1} + T; t_k) - \hat{x}^*(t_{k-1} + T; t_{k-1})\|_P \leq \frac{L^2\beta T e^{L(1-\beta)T}}{L\beta T - 1} \delta$ . By using the Triangle inequality, we have

$$\|\tilde{x}(t_{k-1} + T; t_k)\|_P \leq \|\hat{x}^*(t_{k-1} + T; t_{k-1})\|_P + \frac{L^2\beta T e^{L(1-\beta)T}}{L\beta T - 1} \delta, \quad (26)$$

which implies that  $\|\tilde{x}(t_{k-1} + T; t_k)\|_P \leq \alpha\epsilon + \frac{L^2\beta T e^{L(1-\beta)T}}{L\beta T - 1} \delta$ .

Note from Theorem 1 that the designed triggering level  $\delta = \rho \bar{\lambda}(\sqrt{P}) \left[ e^{L\beta T} \left( \frac{\beta T}{L} - \frac{1}{L^2} \right) + \frac{1}{L^2} \right]$ . In order to steer the candidate state trajectory  $\tilde{x}(t_{k-1} + T; t_k)$  into  $\Omega(\epsilon)$ , one can simply deduce that the following inequality must holds

$$\frac{L^2\beta T e^{L(1-\beta)T}}{L\beta T - 1} \rho \bar{\lambda}(\sqrt{P}) \left[ e^{L\beta T} \left( \frac{\beta T}{L} - \frac{1}{L^2} \right) + \frac{1}{L^2} \right] \leq (1 - \alpha)\epsilon. \quad (27)$$

From (27), it can be also obtained that the maximum bound for disturbance satisfies  $\rho \leq$

$$\frac{(1 - \alpha)\epsilon}{\frac{L^2\beta T e^{L(1-\beta)T}}{L\beta T - 1} \bar{\lambda}(\sqrt{P}) \left[ e^{L\beta T} \left( \frac{\beta T}{L} - \frac{1}{L^2} \right) + \frac{1}{L^2} \right]}.$$

Second, we consider the candidate trajectory  $\tilde{x}(s; t_k)$  for  $s \in [t_{k-1} + T, t_k + T]$ . By using Lemma 1, we can verify that  $\Omega(\epsilon)$  is an invariant set for the closed-loop system  $\dot{\tilde{x}}(s; t_k) =$

$f(\tilde{x}(s; t_k), K(\tilde{x}(s; t_k)))$ . Consequently, we can deduce that  $\dot{V}(\tilde{x}(s; t_k)) \leq -\|\tilde{x}(s; t_k)\|_{Q^*}^2$ . By the virtue of comparison principle for  $s \in [t_{k-1} + T, t_k + T]$ , it follows that

$$V(\tilde{x}(s; t_k)) \leq \epsilon^2 e^{-\frac{\lambda(Q^*)}{\lambda(P)}(s-t_{k-1}-T)}, \quad (28)$$

which indicates that  $V(\tilde{x}(t_k + T; t_k)) \leq \epsilon^2 e^{-\frac{\lambda(Q^*)}{\lambda(P)}(t_k-t_{k-1})}$ . By using Theorem 1, we can have  $\inf(t_k - t_{k-1}) = \beta T$ . To obtain  $\|\tilde{x}(t_k + T; t_k)\|_P \leq \alpha\epsilon$ , it is equivalent to show that  $V(\tilde{x}(t_k + T; t_k)) \leq \alpha^2 \epsilon^2$ . With some calculation, one can obtain  $T \geq -2 \frac{\bar{\lambda}(P)}{\lambda(Q^*)\beta} \ln \alpha$  to guarantee the previous inequality holds. Similar argument can be found in [14].

Third, we show that  $\tilde{x}(s; t_k)$  will satisfy the state constraint (7). For  $s \in (t_k, t_{k-1} + T]$ , one can get

$$\|\tilde{x}(s; t_k)\|_P \leq \|\hat{x}^*(s; t_{k-1})\|_P + \frac{L^2 \beta T e^{L(1-\beta)T}}{L\beta T - 1} \delta, \quad (29)$$

which can be easily derived from (15). Then we need to prove

$$\frac{(t_k + T - s)M + s - t_k}{T} \alpha\epsilon \leq \frac{(t_{k-1} + T - s)M + s - t_{k-1}}{T} \alpha\epsilon + \frac{L^2 \beta T e^{L(1-\beta)T}}{L\beta T - 1} \delta. \quad (30)$$

By some calculation, it can be obtain that  $M \geq \frac{L^2 \beta T e^{L(1-\beta)T}}{L\beta T - 1} \frac{\delta}{\alpha\epsilon} + 1$ . For  $s \in (t_{k-1} + T, t_k + T]$ , it can be derived from (28) that

$$\|\tilde{x}(s; t_k)\|_P \leq \epsilon e^{-\frac{\lambda(Q^*)}{\lambda(P)}(s-t_{k-1}-T)/2}. \quad (31)$$

In order to prove  $\|\tilde{x}(s; t_k)\|_P \leq \frac{(t_k + T - s)M + s - t_k}{T} \alpha\epsilon$ , it is equivalent to show

$$\frac{(t_k + T - s)M + s - t_k}{T} \alpha\epsilon \geq \epsilon e^{-\frac{\lambda(Q^*)}{\lambda(P)}(s-t_{k-1}-T)/2}. \quad (32)$$

For brevity, we denote  $F(s) = \frac{T/\alpha\epsilon e^{-\frac{\lambda(Q^*)}{\lambda(P)}(s-t_{k-1}-T)/2} + t_k - s}{t_k + T - s}$ , and it turns out that  $M \geq F(s)$ .

By evaluating the derivative of  $F(s)$ , it can be verified that  $F'(s)$  is non-positive for  $s \in (t_{k-1} + T, t_k + T]$ , which indicates  $M \geq 1 - \frac{1}{\beta} + \frac{1}{\alpha\beta}$ . Finally, the designing parameter should be set as  $M \geq \max\{\frac{L^2 \beta T e^{L(1-\beta)T}}{L\beta T - 1} \frac{\delta}{\alpha\epsilon} + 1, 1 - \frac{1}{\beta} + \frac{1}{\alpha\beta}\}$  for guaranteeing the satisfaction of the proposed robustness constraint. The proof is completed.  $\square$

**Remark 3.** Note from Theorem 2 that the feasibility can be affected by the prediction horizon  $T$ , the Lipschitz constant  $L$ , and the disturbance bound  $\rho$ . In order to achieve the recursive feasibility, the prediction horizon  $T$  should be lower bounded, and the design parameter  $M$  in (7) should be lower bounded as well. Specifically, a larger  $M$  leads to a larger initial feasible region. It should be also noted that the maximum allowable disturbance can be decided as (27), which

shows that the allowable disturbance and the prediction horizon are correlated to each other. Thus the trade-off between these two parameters must be taken into account when designing the algorithm.

### B. Stability Analysis

In this part, we investigate the closed-loop stability of the proposed integral-type event-triggered RHC. In the following theorem, we mainly analyze the non-increasing properties of the cost function in (8). Due to the existence of the disturbance, it is worthwhile to point out that the closed-loop stability can be achieved to converge to an invariant set. Since we use the RHC configuration, the analysis for stability can be divided into two steps: One is to ensure that the optimal trajectory will enter the terminal set in finite time; the other is to prove that the closed-loop system is stable after the state enters the terminal set  $\Omega(\epsilon)$ .

**Theorem 3.** *Suppose that the assumptions 1 and 2 hold, and the conditions in Theorem 2 are satisfied, then the closed-loop system (9) enters the designed set  $\Omega(\epsilon)$  in finite time and converges to  $\Omega(\bar{\epsilon})$  if the following condition holds:*

$$\begin{aligned} & \frac{\bar{\lambda}(Q)}{\lambda(P)} \frac{L^2 \beta T (1 - \beta) T}{L \beta T - 1} \left[ \frac{L^2 \beta T}{L \beta T - 1} \delta^2 + 2[(1 - \beta)M + \beta] \alpha \epsilon \delta \right] \\ & \leq \frac{\lambda(Q)n}{\bar{\lambda}(P)(n + 1)} \beta T (\alpha \epsilon - \delta)^2, \exists n \in \mathbb{N}. \end{aligned} \quad (33)$$

*Proof.* This theorem will be proved by two steps.

Step 1: For all initial state  $x(t_0) \in \mathcal{X} \setminus \Omega(\epsilon)$ , we aim to show the state trajectory enters  $\Omega(\epsilon)$  in finite time. In this situation, we construct an error term of two Lyapunov functions as follows  $\Delta \tilde{J}(x(s; t_k), u(s; t_k)) := J(\tilde{x}(s; t_k), \tilde{u}(s; t_k)) - J(\hat{x}^*(s; t_{k-1}), \hat{u}^*(s; t_{k-1}))$ . Expanding this term yields

$$\begin{aligned} \Delta \tilde{J}(x(s; t_k), u(s; t_k)) &= \int_{t_k}^{t_k+T} \|\tilde{x}(s; t_k)\|_Q^2 + \|\tilde{u}(s; t_k)\|_R^2 \mathbf{d}s + \|\tilde{x}(t_k + T; t_k)\|_P^2 \\ & - \int_{t_{k-1}}^{t_{k-1}+T} \|\hat{x}^*(s; t_{k-1})\|_Q^2 + \|\hat{u}^*(s; t_{k-1})\|_R^2 \mathbf{d}s - \|\hat{x}^*(t_{k-1} + T; t_{k-1})\|_P^2. \end{aligned} \quad (34)$$

Substituting  $\tilde{u}(s; t_k)$  (12) to the above equation, we can obtain that

$$\begin{aligned} \Delta \tilde{J}(x(s; t_k), u(s; t_k)) &= \int_{t_{k-1}+T}^{t_k+T} \|\tilde{x}(s; t_k)\|_{Q^*}^2 ds \\ &+ \int_{t_k}^{t_{k-1}+T} \|\tilde{x}(s; t_k)\|_Q^2 - \|\hat{x}^*(s; t_{k-1})\|_Q^2 + \|\tilde{u}(s; t_k)\|_R^2 - \|\hat{u}^*(s; t_{k-1})\|_R^2 ds \\ &- \int_{t_{k-1}}^{t_k} \|\hat{x}^*(s; t_{k-1})\|_Q^2 + \|\hat{u}^*(s; t_{k-1})\|_R^2 ds + \|\tilde{x}(t_k + T; t_k)\|_P^2 - \|\hat{x}^*(t_{k-1} + T; t_{k-1})\|_P^2. \end{aligned} \quad (35)$$

Note from Lemma 1 that  $\dot{V}(\tilde{x}(s; t_k)) \leq -\|\tilde{x}(s; t_k)\|_{Q^*}^2$ . Taking integral from  $t_{k-1} + T$  to  $t_k + T$  of the above inequality yields

$$\begin{aligned} \int_{t_{k-1}+T}^{t_k+T} \dot{V}(\tilde{x}(s; t_k)) ds &= \|\tilde{x}(t_k + T; t_k)\|_P^2 - \|\tilde{x}(t_{k-1} + T; t_k)\|_P^2 \\ &\leq - \int_{t_{k-1}+T}^{t_k+T} \|\tilde{x}(s; t_k)\|_{Q^*}^2 ds. \end{aligned} \quad (36)$$

Applying this fact to  $\Delta \tilde{J}(x(s; t_k), u(s; t_k))$ , it can be shown that

$$\begin{aligned} &\Delta \tilde{J}(x(s; t_k), u(s; t_k)) \\ &\leq \int_{t_k}^{t_{k-1}+T} \|\tilde{x}(s; t_k)\|_Q^2 - \|\hat{x}^*(s; t_{k-1})\|_Q^2 ds - \int_{t_{k-1}}^{t_k} \|\hat{x}^*(s; t_{k-1})\|_Q^2 + \|\hat{u}^*(s; t_{k-1})\|_R^2 ds. \end{aligned} \quad (37)$$

To analyze the above inequality, we firstly consider the term

$$A = \int_{t_k}^{t_{k-1}+T} \|\tilde{x}(s; t_k)\|_Q^2 - \|\hat{x}^*(s; t_{k-1})\|_Q^2 ds. \quad (38)$$

By using the triangle inequality, we have

$$A \leq \int_{t_k}^{t_{k-1}+T} \|\tilde{x}(s; t_k) - \hat{x}^*(s; t_{k-1})\|_Q^2 ds + 2 \int_{t_k}^{t_{k-1}+T} \|\tilde{x}(s; t_k) - \hat{x}^*(s; t_{k-1})\|_Q \cdot \|\hat{x}^*(s; t_{k-1})\|_Q ds \quad (39)$$

Then apply Holder inequality, and it follows that

$$\begin{aligned} A &\leq \int_{t_k}^{t_{k-1}+T} \|\tilde{x}(s; t_k) - \hat{x}^*(s; t_{k-1})\|_Q ds \cdot \|\tilde{x}(s; t_k) - \hat{x}^*(s; t_{k-1})\|_Q^\infty \\ &\quad + 2 \int_{t_k}^{t_{k-1}+T} \|\tilde{x}(s; t_k) - \hat{x}^*(s; t_{k-1})\|_Q ds \cdot \|\hat{x}^*(s; t_{k-1})\|_Q^\infty. \end{aligned} \quad (40)$$

Using the result in Corollary 1, it can be easily calculated that

$$A \leq \frac{\bar{\lambda}(Q)}{\underline{\lambda}(P)} \frac{L^2 \beta T (1 - \beta) T}{L \beta T - 1} \delta \left( \frac{L^2 \beta T}{L \beta T - 1} \delta + 2[(1 - \beta)M + \beta] \alpha \epsilon \right). \quad (41)$$

For the other term

$$B = \int_{t_{k-1}}^{t_k} \|\hat{x}^*(s; t_{k-1})\|_Q^2 + \|\hat{u}^*(s; t_{k-1})\|_R^2 ds, \quad (42)$$

it follows that

$$B \geq \int_{t_{k-1}}^{t_k} \|\hat{x}^*(s; t_{k-1}) - x(s; t_{k-1}) + x(s; t_{k-1})\|_Q^2 ds. \quad (43)$$

Since  $x(t_0) \in \mathcal{X} \setminus \Omega(\epsilon)$ , we can have  $B \geq \frac{\lambda(Q)}{\lambda(P)} \beta T (\epsilon - \delta)^2$ . Consequently, it can be obtained that

$$\Delta \tilde{J}(x(s; t_k), u(s; t_k)) \leq A - B \leq -\frac{\lambda(Q)}{\lambda(P)(n+1)} \beta T (\epsilon - \delta)^2 \quad (44)$$

for some positive integer  $n$  if the stability condition (33) is satisfied. Due to the sub-optimality of the designed control  $\tilde{u}(s; t_k)$  at  $t_k$ , we can achieve that the decreasing properties of optimal cost function at  $t_{k-1}$  and  $t_k$  is guaranteed by

$$\Delta J(\hat{x}^*(s; t_k), \hat{x}^*(s; t_k)) \leq -\frac{\lambda(Q)}{\lambda(P)(n+1)} \beta T (\epsilon - \delta)^2, \quad (45)$$

which consequently shows that the optimal cost functional  $J^*$  is decreasing as  $t$  approaches to infinity. Since the nominal state  $\tilde{x}$  stays outside  $\Omega(\epsilon)$ , it can be noted from (45) that the lower bound for the decreasing of optimal functional  $J^*$  is a positive constant. Assume that the nominal state  $\tilde{x}$  cannot converge to the terminal set  $\Omega(\epsilon)$  in finite time, then the optimal functional will decrease to  $-\infty$  as time evolves to infinity, which is a contradiction to the fact that the optimal functional is quadratic. Similar argument can be found in [14], [18].

Step 2: For all initial state  $x(t_0) \in \Omega(\epsilon)$ , we need to prove that the closed-loop system (9) converges to an robustly invariant set  $\Omega(\bar{\epsilon})$ . By following the similar technique proposed in [21], we can obtain the convergence of the closed-loop system by verifying two facts i.e., (C1) the state enters  $\Omega(\bar{\epsilon})$  in finite time and (C2)  $\Omega(\bar{\epsilon})$  is robustly invariant for the system (1). Then the proof can be completed by summarizing Step (1) and Step (2).  $\square$

**Remark 4.** *The inequality (33) shows that the stability can be guaranteed by properly designing the prediction horizon  $T$ , the triggering level  $\delta$ , and the contraction rate for the robustness constraint  $M$ . In addition, the upper bound of the additive disturbance  $\rho$  and the Lipschitz constant  $L$  of the real system model can affect the the decreasing properties of the optimal cost function. Thus it is necessary to take this effect into account while designing the RHC controller for the system in presence of disturbance. Moreover, our theoretical results give an insight about the trade-off of these two designing parameters. Generally speaking, the larger triggering level  $\delta$  leads to less frequent sampling, thus consequently reducing the frequency of operating the computational-consuming optimization task. The larger prediction horizon  $T$  usually provides better control performance due to the fact that longer state evolution is considered*

in the optimization. However, the larger triggering level will cause poorer control performance. Thus the design for the triggering level must take a balance between control performance and computational load.

For a clear view of the aforementioned integral-type event-triggered RHC, we design the event-triggered RHC algorithm as described in Algorithm 1.

---

**Algorithm 1** Integral-type event-triggered RHC

---

- 1: **while**  $x(s; t_k) \notin \Omega(\alpha\epsilon)$  **do**
  - 2:   **if**  $k = 0$  **then**
  - 3:     Solve the Optimization Problem  $\mathcal{P}$
  - 4:   **end if**
  - 5:   **while** The ETM condition (10) is not triggered **do**
  - 6:     Apply optimal control input  $\hat{u}^*(s; t_k)$
  - 7:   **end while**
  - 8:    $k = k + 1$
  - 9:   Solve the Optimization Problem  $\mathcal{P}$  after  $k + 1$  sampling
  - 10: **end while**
- 

#### IV. SIMULATION RESULTS

Consider a nonlinear cart-damper-spring system with the following dynamics:

$$\begin{cases} \dot{x}_1(t) = x_2(t), \\ \dot{x}_2(t) = -\frac{\tau}{M_c} e^{-x_1(t)} x_1(t) - \frac{h_d}{M_c} x_2(t) + \frac{u(t)}{M_c} + \frac{\omega(t)}{M_c}, \end{cases}$$

where  $x_1(t)$  denotes the displacement of the cart,  $x_2(t)$  is the velocity, its mass  $M_c = 1.25$  kg, the nonlinear factor  $\tau = 0.9$  N/m, the damping factor  $h_d = 0.42$  N\*s/m, and the constrained control input  $u(t) \in [-1, 1]$ . For this integral-type event-triggered RHC, we choose the weighted matrices  $Q = [0.1, 0.0; 0.0, 0.1]$  and  $R = 0.1$ . The  $P$  matrix is designed as  $P = [0.5234, -0.1561; -0.1561, 0.2986]$  and the terminal set level is  $\epsilon = 0.03$ . The scaling ratio of the terminal set is  $\alpha = 0.8$ . According to Theorem 1, we choose the minimum inter-execution time as  $\beta T = 1.2$  s. This model along with its parameters is adopted in [14].

In addition,  $T = 2.0$  s and  $M = 20$  are chosen for satisfying the feasibility and stability conditions (21), (22), (33). According to the theoretical results in Theorem 2, it can be calculated



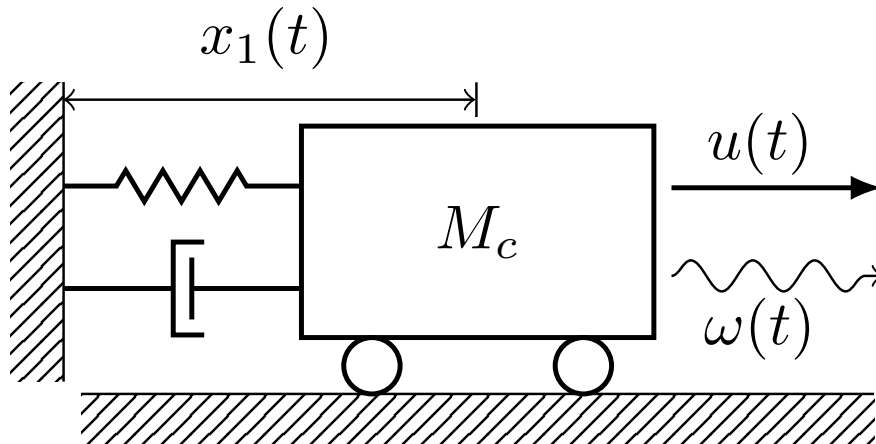


Fig. 2. The schematic illustration of a cart-damper-spring system.

that the maximum allowable disturbance is  $\rho_{MAX} = 0.00039$ . Thus the additive disturbance is set as  $\rho = 0.00031$ . Applying the triggering condition in (10), it can be calculated that the triggering level is  $\delta = 0.000438$ . The initial state of the system is given as  $x_0 = [0.3, -0.20]$ . By using the optimization software [22], the simulation is conducted by implementing the integral-type event-triggered RHC. The trajectory of displacements and velocities of the closed-loop system are illustrated in Fig. 3, where it can be seen that the states enters the terminal set  $\Omega(\epsilon)$  after conducting two online optimizations and two event-triggered samples. In order to show the advantages of the proposed integral-type event-triggered RHC scheme, we also conduct two Monte-Carlo simulations to investigate the performance by comparing it with an event-triggered RHC algorithm proposed in [14]. The results are listed in Table I. From this table, we can see that the integral-type event-triggered RHC can save significant amount of communication resource by performing less frequent event-triggered samplings, which is more efficient than the conventional event-triggered RHC.

## V. CONCLUSION AND FUTURE WORK

In this paper, we have designed an integral-type event-triggered RHC algorithm for nonlinear systems with additive disturbance. The integral-type ETM has shown considerable improvement on avoiding unnecessary communication, thus reducing communication resource. A novel ro-

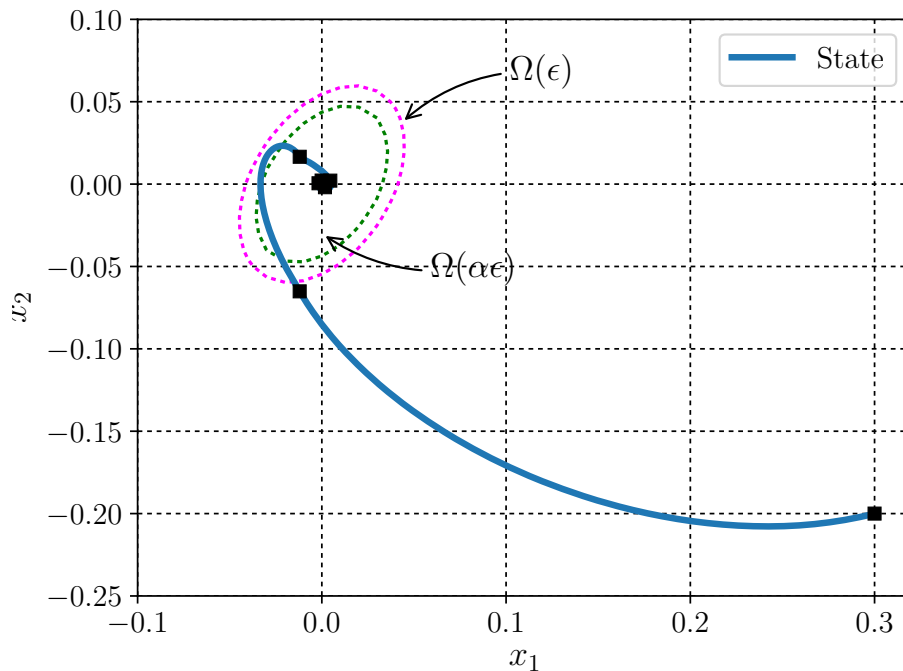


Fig. 3. States Evolution of the closed-loop system (9) driven by integral-type event-triggered RHC (4), where the black squares denotes the event-triggered instants.

TABLE I  
COMPARISON OF EVENT-TRIGGERED SAMPLINGS IN 100 SIMULATIONS.

Algorithm	Average sampling frequency in 12 seconds
ET-RHC [14]	6.46
INTET-RHC	6.19

bustness constraint is also introduced to handle the additive disturbance. For the feasibility and stability of the proposed RHC framework, we have developed several conditions to guarantee these two properties. In addition, we show that the feasibility and stability is subject to the prediction horizon, the disturbance bound, the triggering level, and the contraction rate for the robustness constraint. A simulated example is conducted to show the effectiveness of stabilizing the given nonlinear cart-damper-spring system. Future study will be focused on the output-based event-triggered scheme for RHC control framework and distributed RHC with integral-type event-triggering condition.

## REFERENCES

- [1] K. J. Åström and B. Bernhardsson, “Comparison of riemann and lebesque sampling for first order stochastic systems,” in *Proceedings of the 41st IEEE Conference on Decision and Control, 2002*, vol. 2. IEEE, 2002, pp. 2011–2016.
- [2] J. K. Yook, D. M. Tilbury, and N. R. Soparkar, “Trading computation for bandwidth: Reducing communication in distributed control systems using state estimators,” *IEEE transactions on control systems technology*, vol. 10, no. 4, pp. 503–518, 2002.
- [3] W. Heemels, J. Sandee, and P. Van Den Bosch, “Analysis of event-driven controllers for linear systems,” *International journal of control*, vol. 81, no. 4, pp. 571–590, 2008.
- [4] P. Tabuada, “Event-triggered real-time scheduling of stabilizing control tasks,” *IEEE Transactions on Automatic Control*, vol. 52, no. 9, pp. 1680–1685, 2007.
- [5] W. Heemels, M. Donkers, and A. R. Teel, “Periodic event-triggered control based on state feedback,” in *Decision and Control and European Control Conference (CDC-ECC), 2011 50th IEEE Conference on*. IEEE, 2011, pp. 2571–2576.
- [6] W. Heemels and M. Donkers, “Model-based periodic event-triggered control for linear systems,” *Automatica*, vol. 49, no. 3, pp. 698–711, 2013.
- [7] W. Heemels, M. Donkers, and A. R. Teel, “Periodic event-triggered control for linear systems,” *IEEE Transactions on Automatic Control*, vol. 58, no. 4, pp. 847–861, 2013.
- [8] J. Lunze and D. Lehmann, “A state-feedback approach to event-based control,” *Automatica*, vol. 46, no. 1, pp. 211–215, 2010.
- [9] M. Donkers and W. Heemels, “Output-based event-triggered control with guaranteed  $\mathcal{L}_\infty$ -gain and improved and decentralized event-triggering,” *IEEE Transactions on Automatic Control*, vol. 57, no. 6, pp. 1362–1376, 2012.
- [10] S. Mousavi and H. Marquez, “Integral-based event triggering controller design for stochastic LTI systems via convex optimisation,” *International Journal of Control*, vol. 89, no. 7, pp. 1416–1427, 2016.
- [11] D. Lehmann, E. Henriksson, and K. H. Johansson, “Event-triggered model predictive control of discrete-time linear systems subject to disturbances,” in *Control Conference (ECC), 2013 European*. IEEE, 2013, pp. 1156–1161.
- [12] F. D. Brunner, W. Heemels, and F. Allgower, “Robust event-triggered MPC with guaranteed asymptotic bound and average sampling rate,” *IEEE Transactions on Automatic Control*, 2017.
- [13] A. Eqtami, D. V. Dimarogonas, and K. J. Kyriakopoulos, “Novel event-triggered strategies for model predictive controllers,” in *Decision and Control and European Control Conference (CDC-ECC), 2011 50th IEEE Conference on*. IEEE, 2011, pp. 3392–3397.
- [14] H. Li and Y. Shi, “Event-triggered robust model predictive control of continuous-time nonlinear systems,” *Automatica*, vol. 50, no. 5, pp. 1507–1513, 2014.
- [15] A. Eqtami, D. V. Dimarogonas, and K. J. Kyriakopoulos, “Event-triggered strategies for decentralized model predictive controllers,” *IFAC Proceedings Volumes*, vol. 44, no. 1, pp. 10068–10073, 2011.
- [16] K. Hashimoto, S. Adachi, and D. V. Dimarogonas, “Self-triggered model predictive control for nonlinear input-affine dynamical systems via adaptive control samples selection,” *IEEE Transactions on Automatic Control*, vol. 62, no. 1, pp. 177–189, 2017.
- [17] P. Varutti, B. Kern, T. Faulwasser, and R. Findeisen, “Event-based model predictive control for networked control systems,” in *Decision and Control, 2009 held jointly with the 2009 28th Chinese Control Conference. CDC/CCC 2009. Proceedings of the 48th IEEE Conference on*. IEEE, 2009, pp. 567–572.
- [18] H. Chen and F. Allgöwer, “A quasi-infinite horizon nonlinear model predictive control scheme with guaranteed stability,” *Automatica*, vol. 34, no. 10, pp. 1205–1217, 1998.

- [19] H. Li and Y. Shi, “Distributed model predictive control of constrained nonlinear systems with communication delays,” *Systems & Control Letters*, vol. 62, no. 10, pp. 819–826, 2013.
- [20] H. Michalska and D. Mayne, “Robust receding horizon control of constrained nonlinear systems,” *IEEE Transactions on Automatic Control*, vol. 38, pp. 1623–1633, 1993.
- [21] H. Li and Y. Shi, “Robust distributed model predictive control of constrained continuous-time nonlinear systems: A robustness constraint approach,” *IEEE Transactions on Automatic Control*, vol. 59, no. 6, pp. 1673–1678, 2014.
- [22] A. Wächter and L. T. Biegler, “On the implementation of an interior-point filter line-search algorithm for large-scale nonlinear programming,” *Mathematical programming*, vol. 106, no. 1, pp. 25–57, 2006.